Journal of Photochemistry and Photobiology A: Chemistry 207 (2009) 94–101

Contents lists available at ScienceDirect

Journal of Photochemistry and Photobiology A: Chemistry

journal homepage: www.elsevier.com/locate/jphotochem

Synthesis, characterisation and luminescence properties of carbazole-containing platinum(II) and palladium(II) alkynyl complexes

Chi-Hang Tao, Nianyong Zhu, Vivian Wing-Wah Yam*

Centre for Carbon-Rich Molecular and Nanoscale Metal-Based Materials Research, and Department of Chemistry, The University of Hong Kong, Pokfulam Road, Hong Kong, PR China

ARTICLE INFO

Article history:
Available online 21 November 2008

Dedicated to Prof. Haruo Inoue on the occasion of his 60th birthday.

Keywords:
Luminescence
Platinum(II) complexes
Palladium(II) complexes
Metal alkynyls
Carbazole

ABSTRACT

A series of luminescent carbazole-containing palladium(II) and platinum(II) alkynyl complexes has been successfully synthesized and characterized. Through a systematic comparison study, the emission of the platinum(II) bis-alkynyl complexes has been assigned to originate from an admixture of ^{3}IL/^{3}MLCT excited states with predominantly IL character.

1. Introduction

The research of organic polymeric materials is undoubtedly one of the most active areas of research in chemistry, especially during the past decade, due to their intriguing physical properties, ease of fabrication and wide range of applications. The search for new multifunctional materials has boosted the development of copolymers/block copolymers, by which different components with desired properties can be brought together in an easy and rapid manner.

Among the vast library of different monomers with various unique properties, carbazole is probably amongst one of the most extensively studied. Developments based on the use of carbazole as the building block for the synthesis of branched molecules, oligomers, polymers or even dendrimers have recently been reported, however, most of them are confined to organic-based systems [1–9].

Carbazole can be conveniently functionalised at the 3-, 6-, and 9-positions with various functional groups, and thus many different derivatives of carbazole-containing polymers, with carbazole as part of the main chain or constituting as pendant groups in the side chains of copolymers or block copolymers, have been synthesized and studied [10–14]. It is well known that carbazole compounds possess interesting properties, such as photoconductivity [15], second order nonlinearity [16], photorefractivity [1], hole transport properties [3,7,17–23] and luminescent properties [3,5,7,9]. All these advantages make carbazoles promising building blocks for the synthesis of new multifunctional materials.

In recent years, much attention have focused on the development and optimisation of organic light emitting diodes (OLEDs). Carbazole has been extensively incorporated into different organic systems to enhance their hole transport properties as well as to tune the colour of emission [24]. As an example, the well-known poly(*N*-vinylcarbazole) (PVK), doped with other luminescent organic dyes, has been shown to display remarkable enhancement in luminescence efficiency [17]. In contrast to carbazole-containing organic polymers, carbazole-containing coordination compounds were relatively less explored [25–30]. It was only until 1999 that Ribou et al. reported the first carbazole-containing coordination compounds, $[(NH_3)_5Ru(3\text{-}(2\text{-}(4\text{-pyridyl})ethylenyl)carbazole)](PF_6)_2$ and $[Ru(trpy)(bpy)(3\text{-}(2\text{-}(4\text{-pyridyl})ethylenyl)carbazole)](PF_6)_2$, with studies of their optical and electrochemical properties [25].

Organometallic polymeric materials have also attracted increasing interest since the first soluble platinum(II) and palladium(II) polyynyl complexes were reported [31,32]. Kim and co-workers reported the polymerization of distyryldiphenyltin and 3,6-dibromo-9-(2-ethylhexyl)carbazole to yield a π-conjugated tin-based alternating copolymer via the Heck reaction. The copolymer used for the fabrication of LED emitted in the blue region with very low operating voltage [28], which further highlighted the advantages of the use of carbazole moieties in OLEDs.

The studies on platinum-containing polymers have been one of the fast growing sectors in the field of metallopolymer.

* Corresponding author. Tel.: +852 2859 2153; fax: +852 2857 1586.
E-mail address: wwyam@hku.hk (V.W.-W. Yam).

1010-6030/$ – see front matter © 2008 Elsevier B.V. All rights reserved.
doi:10.1016/j.jphotochem.2008.11.006

Various platinum complexes, oligomers and metallopolymers with different spacers and chain lengths have been reported by Lewis [33,34], Raithby [35–38], Schanze [39–41], Gladysz [42–44], Wong [27,45,46] and others [47–49]. The synthesis of carbazole-containing platinum(II) polyynes and the studies of their photoluminescent properties have been reported recently [27]. On the other hand, recent works by various researchers have shown that platinum(II) alkynyl complexes, other than polymeric materials, are promising and versatile building blocks for the construction of novel multinuclear luminescent complexes [39,47,49–54]. In addition, the employment of platinum(II) alkynyl complexes and polymers in the field of nonlinear optics, such as optical limiting, two-photon absorption and two-photon induced luminescence, have drawn particular attention [45,55–58]. As an extension of our work on luminescent metal alkynyl systems [53,54,59–65], a series of carbazole-containing chloropalladium(II), [{ClPd(PEt_3)$_2$C≡C}$_2$-3,6-^{n}BuCarb-9] (**1**), and platinum(II) bis-alkynyl complexes, [{RC≡CPt(PEt_3)$_2$C≡C}$_2$-3,6-^{n}BuCarb-9] [R = $C_6H_4OCH_3$-4 (**2**), $C_6H_4CH_3$-4 (**3**), $C_6H_4CF_3$-4 (**4**) and 1-pyrenyl (Pyr) (**5**)] have been synthesized. Through the variation of the metal centres as well as the nature of the coordinating alkynyl ligands, insights into the spectroscopic origin of the electronic absorption and emission properties of this unique class of compounds are provided.

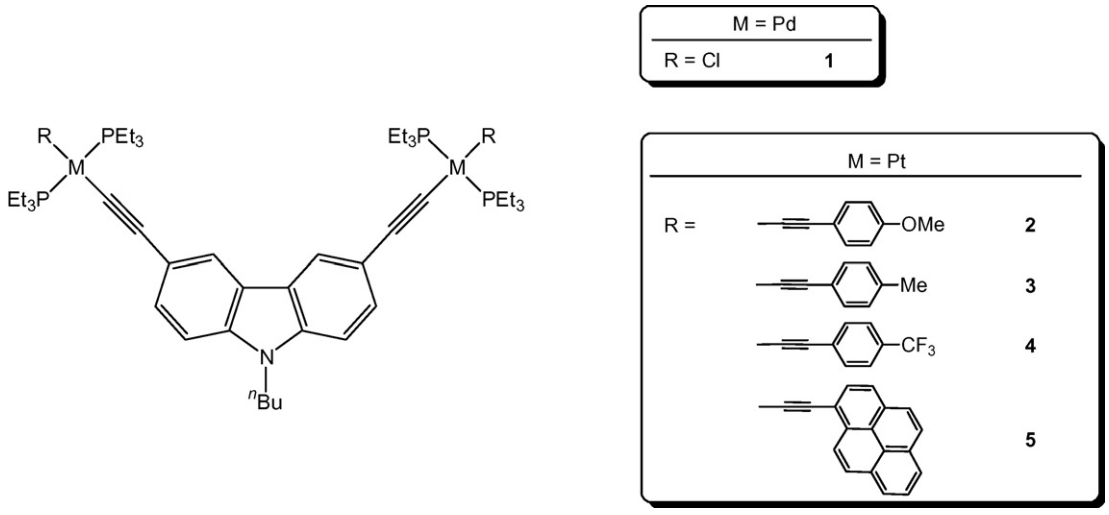

2. Experimental/materials and methods

2.1. Materials and reagents

Diethynyl-3-6-butylcarbazole-9 ((HC≡C)$_2$-3,6-^{n}BuCarb-9) [4], *trans*-[Pd(PEt_3)$_2$Cl$_2$] [66], and [{ClPt(PEt_3)$_2$C≡C}$_2$-3,6-^{n}BuCarb-9] [54] were synthesized according to literature procedures. *trans*-[Pt(PEt_3)$_2$Cl$_2$] (Aldrich, 98%), 1-ethynyl-4-methoxybenzene (Maybridge), 1-ethynyltoluene (GFS, 98%), 1-ethynyl-4-trifluoromethylbenzene (Aldrich, 97%) and 1-ethynylpyrene (Lancaster, 96%) were purchased and used as received. All amines were distilled over potassium hydroxide and stored in the presence of potassium hydroxide prior to use. All other solvents and reagents were of analytical grade and used as received.

2.2. Physical measurements and instrumentation

UV–vis spectra were obtained on a Hewlett-Packard 8452A diode array spectrophotometer, IR spectra as KBr discs on a Bio-Rad FTS-7 Fourier-transform infrared spectrophotometer (4000–400 cm^{-1}), and steady state excitation and emission spectra on a Spex Fluorolog-2 Model F 111 fluorescence spectrophotometer equipped with a Hamamatsu R-928 photomultiplier tube. Low-temperature (77 K) spectra were recorded by using an optical Dewar sample holder. ^{1}H NMR spectra were recorded on a Bruker DPX-300 (300 MHz) Fourier-transform NMR spectrometer, while ^{31}P{^{1}H} NMR spectra were recorded on either a Bruker DPX-300 or a Bruker DPX-500 Fourier-transform NMR spectrometer. Chemical shifts (δ ppm) of ^{1}H NMR spectra were recorded relative to tetramethylsilane (Me_4Si), while that of ^{31}P NMR spectra were recorded relative to 85% H_3PO_4. Positive ion FAB mass spectra were recorded on a Finnigan MAT95 mass spectrometer. Elemental analyses of the new complexes were performed on a Carlo Erba 1106 elemental analyzer at the Institute of Chemistry, Chinese Academy of Sciences.

All solutions for photophysical studies were degassed on a high vacuum line in a two-compartment cell consisting of a 10 mL Pyrex bulb and a 1-cm path length quartz cuvette, and sealed from the atmosphere by a Bibby Rotaflo HP6 Teflon stopper. The solutions were subjected to at least four freeze-pump-thaw cycles. Emission lifetime measurements were performed using a conventional laser system. The excitation source used was a 355-nm output (third harmonic) from a Spectra-Physics Quanta-Ray Q-switched GCR-150-10 pulsed Nd–YAG laser. Luminescence decay signals were detected by a Hamamatsu R928 PMT and recorded on a Tektronix Model TDS-620 A (500 MHz, 2 GS/s) digital oscilloscope, and the data were analysed by using a program for exponential fits.

Cyclic voltammetric measurements were performed by using a CH Instruments, Inc. model CHI 750 A Electrochemical Analyser. Electrochemical measurements were performed in dichloromethane solutions with 0.1 M ^{n}Bu$_4$NPF$_6$ (TBAH) as the supporting electrolyte at room temperature. The reference electrode was an Ag/AgNO$_3$ (0.1 M in acetonitrile) electrode and the working electrode was a glassy carbon electrode (CH Instruments, Inc.) with a platinum wire as the counter electrode. The working electrode surface was first polished with 1 μm alumina slurry (Linde) on a microcloth (Buehler Co.). It was then rinsed with ultra-pure deionised water and sonicated in a beaker containing ultra-pure water for 5 min. The polishing and sonicating steps were repeated twice and then repeated twice with 0.3 μm alumina slurry (Linde). The working electrode was finally rinsed under a stream of ultra-pure deionised water. The ferrocenium/ferrocene couple ($FeCp_2^{+/0}$) was used as the internal reference. All solutions for electrochemical studies were deaerated with pre-purified argon gas prior to measurements.

2.3. Synthesis of carbazole-containing platinum(II) and palladium(II) alkynyl complexes

2.3.1. [{ClPd(PEt$_3$)$_2$C≡C}$_2$-3,6-^{n}BuCarb-9] (**1**)

trans-[Pd(PEt$_3$)$_2$Cl$_2$] (1.000 g, 2.42 mmol) was dissolved in HNEt$_2$ (60 mL) containing CuCl (3.8 mg, 0.038 mmol), which was followed by the addition of (HC≡C)$_2$-3,6-^{n}BuCarb-9 (171 mg, 0.628 mmol), and the reaction mixture was stirred for 3 h at room temperature. The white organic ammonium salt formed during the course of the reaction was then filtered off and the solvent was removed under reduced pressure. Dichloromethane was added to dissolve the yellow residue and the solution was washed successively with aqueous ammonium chloride solution and deionised water to remove the copper(I) catalyst. The organic layer was then dried over anhydrous $MgSO_4$, filtered, and reduced in volume under reduced pressure. The residue was passed through a column of aluminum oxide (basic, 50–200 μm) using dichloromethane–petroleum ether (1:1, v/v) as the eluent to remove the excess *trans*-[Pd(PEt$_3$)$_2$Cl$_2$]. The dinuclear complex **1** was eluted with dichloromethane and subsequent removal of the solvent gave **1** as a very pale yellow solid. Recrystallisation from dichloromethane–*n*-hexane afforded **1** as pale yellow crystals. Yield, 430 mg, 67%. ^{1}H NMR ($CDCl_3$, 298 K, 400 MHz): δ 0.92 (t, J_{HH} = 7.0 Hz, 3H, –NCH$_2$CH$_2$CH$_2$C*H*$_3$), 1.2–1.3 (m, 38H, –PCH$_2$C*H*$_3$ and –NCH$_2$CH$_2$C*H*$_2$–), 1.81 (quintet, J_{HH} = 7.0 Hz, 2H, –NCH$_2$C*H*$_2$–), 2.05–2.15 (m, 24H, –CH$_2$P), 4.22 (t, J_{HH} = 7.0 Hz, 2H, NCH$_2$–), 7.23 (d, J_{HH} = 8.5 Hz, 2H, H's at 1-position of carbazole), 7.34 (dd, J_{HH} = 8.5, 1.7 Hz, 2H, H's at 2-position of carbazole), 7.93 (d, J_{HH} = 1.7 Hz, 2H, H's at 4-position of carbazole). ^{31}P{^{1}H} NMR ($CDCl_3$, 298 K, 162 MHz): δ 18.2. IR (KBr disc, ν (cm^{-1})): 2114 m ν(C≡C). Positive FAB-MS: 1025 [M]$^+$, 907 [M–PEt$_3$]$^+$. Elemental analyses, found: C, 51.7%; H, 7.33%; N, 1.37%; Anal. calcd. for **1**: C, 51.5%; H, 7.34%; N, 1.37%.

2.3.2. [{MeOC$_6$H$_4$C≡CPt(PEt$_3$)$_2$C≡C}$_2$-3,6-^{n}BuCarb-9] (**2**)

This was synthesized according to a modified literature procedure for the related alkynyl platinum(II) complexes [53]. [{ClPt(PEt$_3$)$_2$C≡C}$_2$-3,6-^{n}BuCarb-9] (200 mg, 0.166 mmol) and 1-ethynyl-4-methoxybenzene (90 mg, 0.68 mmol) were dissolved in a mixture of THF (20 mL) and diethylamine (10 mL). To this reaction mixture was added CuCl (5 mg) as a catalyst. The yellow mixture was then stirred overnight at room temperature. The white organic ammonium salt formed during the course of the reaction was filtered off and the solvent removed under reduced pressure. The resulting greenish yellow gummy residue was then redissolved in dichloromethane and washed successively with brine, deionised water and dried over anhydrous Na_2SO_4. This was then filtered, and the solvent was removed under reduced pressure. The yellow residue was subjected to column chromatography on basic aluminum oxide (50–200 μm) using dichloromethane as the eluent. Subsequent recrystallisation of the crude product with dichloromethane–*n*-hexane afforded **2** as a very pale yellow solid. Yield, 143 mg, 62%. ^{1}H NMR ($CDCl_3$, 298 K, 400 MHz): δ 0.93 (t, J_{HH} = 6.8 Hz, 3H, –NCH$_2$CH$_2$CH$_2$C*H*$_3$), 1.2–1.4 (m, 38H, –PCH$_2$C*H*$_3$ and –NCH$_2$CH$_2$C*H*$_2$–), 1.81 (quintet, J_{HH} = 6.8 Hz, 2H, –NCH$_2$C*H*$_2$–), 2.2–2.3 (m, 24H, –CH$_2$P), 3.78 (s, 6H, –OMe), 4.22 (t, J_{HH} = 6.8 Hz, 2H, NCH$_2$–), 6.77 (d, J_{HH} = 8.0 Hz, 4H, C$_6$*H*$_4$OMe), 7.20 (d, J_{HH} = 8.0 Hz, 6H, H's at 1-position of carbazole and C$_6$*H*$_4$OMe), 7.38 (dd, 2H, J_{HH} = 8.0, 1.7 Hz, H's at 2-position of carbazole), 7.96 (d, J_{HH} = 1.7 Hz, 2H, H's at 4-position of carbazole). ^{31}P{^{1}H} NMR ($CDCl_3$, 298 K, 162 MHz): δ 11.1 (J_{Pt-P} = 2371 Hz). IR (KBr disc, ν (cm^{-1})): 2102 m ν(C≡C). Positive FAB-MS: 1394 [M+1]$^+$. Elemental analyses, found: C, 53.5%; H, 6.43%; N, 0.97%; Anal. calcd. for **2**: C, 53.4%; H, 6.43%; N, 1.00%.

2.3.3. [{MeC$_6$H$_4$C≡CPt(PEt$_3$)$_2$C≡C}$_2$-3,6-^{n}BuCarb-9] (**3**)

The procedure was similar to that for **2** except that 1-ethynyltoluene (79 mg, 0.68 mmol) was used instead of 1-ethynyl-4-methoxybenzene. Yield, 147 mg, 65%. ^{1}H NMR ($CDCl_3$, 298 K, 400 MHz): δ 0.93 (t, J_{HH} = 6.8 Hz, 3H, –NCH$_2$CH$_2$CH$_2$C*H*$_3$), 1.2–1.4 (m, 38H, –PCH$_2$C*H*$_3$ and –NCH$_2$CH$_2$C*H*$_2$–), 1.81 (quintet, J_{HH} = 6.8 Hz, 2H, –NCH$_2$C*H*$_2$–), 2.2–2.3 (m, 24H, –CH$_2$P), 2.30 (s, 6H, C$_6$H$_4$*Me*$_3$), 4.22 (t, J_{HH} = 6.8 Hz, 2H, NCH$_2$–), 7.02 (d, J_{HH} = 8.0 Hz, 4H, C$_6$*H*$_4$Me), 7.20 (d, J_{HH} = 8.0 Hz, 6H, H's at 1-position of carbazole and C$_6$H$_4$Me), 7.38 (dd, 2H, J_{HH} = 8.0, 1.7 Hz, H's at 2-position of carbazole), 7.96 (d, J_{HH} = 1.7 Hz, 2H, H's at 4-position of carbazole). ^{31}P{^{1}H} NMR ($CDCl_3$, 298 K, 162 MHz): δ 11.0 (J_{Pt-P} = 2380 Hz). IR (KBr disc, ν (cm^{-1})): 2103 s ν(C≡C). Positive FAB-MS: 1362 [M+1]$^+$. Elemental analyses, found: C, 54.4%; H, 6.56%; N, 1.02%; Anal. calcd. for **3**: C, 54.7%; H, 6.58%; N, 1.03%.

2.3.4. [{F$_3$CC$_6$H$_4$C≡CPt(PEt$_3$)$_2$C≡C}$_2$-3,6-^{n}BuCarb-9] (**4**)

The procedure was similar to that for **2** except that 1-ethynyl-4-trifluoromethylbenzene (116 mg, 0.68 mmol) was used instead of 1-ethynyl-4-methoxybenzene. Yield, 144 mg, 59%. ^{1}H NMR ($CDCl_3$, 298 K, 400 MHz): δ 0.93 (t, J_{HH} = 6.8 Hz, 3H, –NCH$_2$CH$_2$CH$_2$C*H*$_3$), 1.2–1.4 (m, 38H, –PCH$_2$C*H*$_3$ and –NCH$_2$CH$_2$C*H*$_2$–), 1.81 (quintet, J_{HH} = 6.8 Hz, 2H, –NCH$_2$C*H*$_2$–), 2.2–2.3 (m, 24H, –CH$_2$P), 2.30 (s, 6H, C$_6$H$_4$*Me*$_3$), 4.22 (t, J_{HH} = 6.8 Hz, 2H, NCH$_2$–), 6.77 (d, J_{HH} = 8.8 Hz, 4H, C$_6$*H*$_4$CF$_3$), 7.20 (d, J_{HH} = 8.0 Hz, 6H, H's at 1-position of carbazole), 7.23 (d, J_{HH} = 8.8 Hz, 4H, C$_6$*H*$_4$CF$_3$), 7.38 (dd, 2H, J_{HH} = 8.0, 1.7 Hz, H's at 2-position of carbazole), 7.95 (d, J_{HH} = 1.7 Hz, 2H, H's at 4-position of carbazole). ^{31}P{^{1}H} NMR ($CDCl_3$, 298 K, 162 MHz): δ 11.2 (J_{Pt-P} = 2397 Hz). IR (KBr disc, ν (cm^{-1})): 2102 m ν(C≡C). Positive FAB-MS: 1470 [M+1]$^+$. Elemental analyses, found: C, 50.4%; H, 5.71%; N, 0.97%; Anal. calcd. for **4**: C, 50.6%; H, 5.69%; N, 0.95%.

2.3.5. [{PyrC≡CPt(PEt$_3$)$_2$C≡C}$_2$-3,6-^{n}BuCarb-9] (**5**)

The procedure was similar to that for **2** except that 1-ethynylpyrene was used instead of 1-ethynyl-4-methoxybenzene. Yield, 137 mg, 52%. ^{1}H NMR ($CDCl_3$, 298 K, 400 MHz): δ 0.94 (t, J_{HH} = 6.8 Hz, 3H, –NCH$_2$CH$_2$CH$_2$C*H*$_3$), 1.2–1.4 (m, 38H, –PCH$_2$C*H*$_3$ and –NCH$_2$CH$_2$C*H*$_2$–), 1.83 (quintet, J_{HH} = 6.8 Hz, 2H, –NCH$_2$C*H*$_2$–), 2.2–2.3 (m, 24H, –CH$_2$P), 4.24 (t, J_{HH} = 6.8 Hz, 2H, NCH$_2$–), 7.24 (d, J_{HH} = 8.6 Hz, 2H, H's at 1-position of carbazole), 7.43 (dd, J_{HH} = 8.6, 1.7 Hz, 2H, H's at 2-position of carbazole), 7.92 (d, J_{HH} = 1.7 Hz, 2H, H's at 4-position of carbazole); 7.94–8.14 (m, 18H, H's at 4-position of carbazole and H's on the Pyr moieties), 8.72 (d, 2H, J_{HH} = 11.0 Hz, aromatic H's on the Pyr moieties). ^{31}P{^{1}H} NMR ($CDCl_3$, 298 K, 162 MHz): δ 11.7 (J_{Pt-P} = 2381 Hz). IR (KBr disc, ν (cm^{-1})): 2084 s ν(C≡C). Positive FAB-MS: 1582 [M]$^+$, 1356 [M–C≡CPyr]$^+$. Elemental analyses, found: C, 60.9%; H, 5.91%; N, 0.90%; Anal. calcd. for **5**: C, 60.7%; H, 5.92%; N, 0.89%.

2.4. Crystal structure determination

Single crystals of [{ClPd(PEt$_3$)$_2$C≡C}$_2$-3,6-^{n}BuCarb-9] (**1**) suitable for X-ray diffraction studies were grown by slow evaporation of a dichloromethane–ethanol solution containing the complex. Single crystals of [{PyrC≡CPt(PEt$_3$)$_2$C≡C}$_2$-3,6-^{n}BuCarb-9] (**5**) were grown by slow diffusion of *n*-pentane vapour into a concentrated benzene solution of the complex.

Crystal data for [{ClPd(PEt$_3$)$_2$C≡C}$_2$-3,6-^{n}BuCarb-9] (**1**): [C$_{44}$H$_{75}$Cl$_2$NP$_4$Pd$_2$]·CH$_3$CH$_2$OH; formula weight = 1071.7, triclinic, space group $P\bar{1}$, a = 10.358(2) Å, b = 15.116(3) Å, c = 19.505(4) Å, α = 106.16(3)°, β = 101.43(3)°, γ = 99.68(3)°, V = 2793.0(10) Å^3, Z = 2, D_c = 1.273 g cm^{-3}, μ(Mo Kα) = 0.884 mm^{-1}, F(0 0 0) = 1116, T = 301 K. A crystal of dimensions 0.7 mm × 0.4 mm × 0.1 mm mounted in a glass capillary with mother liquor was used for data collection at 301 K on a MAR diffractometer with a 300 mm image plate detector using graphite monochromatized Mo Kα radiation

(λ = 0.71073 Å). Data collection was made with 2° oscillation steps of φ, 5 min exposure time and scanner distance at 120 mm. 100 images were collected. The images were interpreted and intensities integrated using the *DENZO* program [67]. The structure was solved by direct methods employing the *SHELXS97* program [68] on a PC and the space group was temporarily set to be *P*1. Four Pd atoms were located according to the direct methods, then the space group was transformed into centric $P\bar{1}$. Positions of other non-hydrogen atoms were found after successful refinement by full-matrix least-squares using the *SHELXL97* program [69] on a PC. The ethyl groups of PEt_3 ligands have relatively high thermal parameters and those of one PEt_3 ligand were treated with disorder. One ethanol solvent molecule was also located. According to the *SHELXL97* program [69], all 6590 independent reflections (R_{int} equal to 0.0315, 4026 reflections larger than $4\sigma(F_o)$, where $R_{int} = \sum |F_o^2 - F_o^2(\text{mean})| / \sum [F_o^2]$) from a total of 12668 reflections participated in the full-matrix least-squares refinement against F^2. These reflections were in the range $-11 \le h \le 11$, $-17 \le k \le 17$, $-22 \le l \le 22$ with $2\theta_{max}$ equal to 49.50°. One crystallographic asymmetric unit consists of one formula unit, including one ethanol solvent molecule. In the final stage of least-squares refinement, atoms of ethyl groups and ethanol solvent molecule were refined isotropically, and other non-hydrogen atoms were refined anisotropically. The hydrogen atoms (except those on ethanol and disordered ethyl groups) were generated by the *SHELXL97* program [69]. The positions of hydrogen atoms were calculated based on the riding mode with thermal parameters equal to 1.2 times that of the associated C atoms, and participated in the calculation of final *R*-indices. Since the structure refinements are against F^2, *R*-indices based on F^2 are larger than (more than double) those based on *F*. For comparison with older refinements based on *F* and an OMIT threshold, a conventional index R_1 based on observed *F* values larger than $4\sigma(F_o)$ was also given (corresponding to intensity $\ge 2\sigma(I)$). $wR_2 = \{\sum [w(F_o^2 - F_o^2)^2] / \sum [w(F_o^2)^2]\}^{1/2}$, $R_1 = \sum ||F_o| - |F_c|| / \Sigma |F_o|$. The Goodness of Fit is always based on F^2: GooF $= S = \{\sum [w(F_o^2 - F_c^2)^2] / (n-p)\}^{1/2}$, where *n* is the number of reflections and *p* is the total number of parameters refined. The weighting scheme is: $w = 1/[\sigma^2(F_o^2) + (aP)^2 + bP]$, where *P* is $[2F_c^2 + \max(F_o^2, 0)]/3$. Convergence $((\Delta/\sigma)_{max} = 0.001$, av. 0.001) for 382 variable parameters by full-matrix least-squares refinement on F^2 reaches to $R_1 = 0.0764$ and $wR_2 = 0.2225$ with a goodness-of-fit of 0.960, the parameters *a* and *b* for weighting scheme are 0.1748 and 0.0. The final difference Fourier map shows maximum rest peaks and holes of 0.739 and −0.493 eÅ^{-3}, respectively.

Crystal data for [{PyrC≡CPt(PEt_3)$_2$C≡C}$_2$-3,6-^{n}BuCarb-9] (**5**): $[C_{80}H_{93}NP_4Pt_2]\cdot 1/2C_6H_6$; formula weight = 1621.67, triclinic, space group $P\bar{1}$ (No. 2), *a* = 10.016(2) Å, *b* = 21.140(4) Å, *c* = 21.461(4) Å, α = 70.27(3)°, β = 89.06(3)°, γ = 88.41(3)°, *V* = 4275.6(14) Å^3, *Z* = 2, D_c = 1.260 g cm^{-3}, ((Mo K() = 3.381 mm^{-1}, *F*(0 0 0) = 1634, *T* = 253 K. A crystal of dimensions 0.60 mm × 0.20 mm × 0.08 mm mounted in a glass capillary was used for data collection at 253 K on a MAR diffractometer with a 300 mm image plate detector using graphite monochromatized Mo K(radiation ((= 0.71073 Å). Data collection was made with 2° oscillation steps of (, 600 s exposure time and scanner distance at 120 mm. 100 images were collected. The images were interpreted and intensities integrated using the *DENZO* program [67]. The structure was solved by direct methods employing the *SIR-97* program [70] on a PC. Pt, P and many non-hydrogen atoms were located according to the direct methods and the successive least-squares Fourier cycles. Positions of other non-hydrogen atoms were found after successful refinement by full-matrix least-squares using the *SHELXL97* program [69] on a PC. Restraints were applied to one triethylphosphine, assuming similar P–C, P···C and C–C bond lengths or distances, respectively. According to the *SHELXL97* program [69], all 9362 independent reflections (R_{int} equal to 0.0500, 5597 reflections larger than $4((F_o)$, where $R_{int} = \sum |F_o^2 - F_o^2(\text{mean})| / \sum [F_o^2]$) from a total of 18 279 reflections participated in the full-matrix least-squares refinement against F^2. These reflections were in the range $-10 \le h \le 10$, $-23 \le k \le 23$, $-22 \le l \le 23$ with $2(_{max}$ equal to 49.00°. One crystallographic asymmetric unit consists of one formula unit, including half benzene solvent molecule. In the final stage of least-squares refinement, C atoms of triethylphosphine and C atoms of benzene were refined isotropically, and other non-hydrogen atoms were refined anisotropically. Hydrogen atoms were generated by the *SHELXL97* program [69]. The positions of hydrogen atoms were calculated based on the riding mode with thermal parameters equal to 1.2 times that of the associated C atoms, and participated in the calculation of final *R*-indices. Since the structure refinements are against F^2, *R*-indices based on F^2 are larger than (more than double) those based on *F*. For comparison with older refinements based on *F* and an OMIT threshold, a conventional index R_1 based on observed *F* values larger than $4\sigma(F_o)$ is also given (corresponding to Intensity $\ge 2((I))$. $wR_2 = \{\sum [w(F_o^2 - F_o^2)^2] / \sum [w(F_o^2)^2]\}^{1/2}$, $R_1 = \Sigma ||F_o| - |F_c|| / \Sigma |F_o|$. The Goodness of Fit is based on F^2: GooF = $S = \{\sum [w(F_o^2 - F_c^2)^2] / (n-p)\}^{1/2}$, where *n* is the number of reflections and *p* is the total number of parameters refined. The weighting scheme is: $w = 1/[\sigma^2(F_o^2) + (aP)^2 + bP]$, where *P* is $[2F_c^2 + \max(F_o^2, 0)]/3$. Convergence $((((/\sigma)_{max} = 0.001$, av. 0.001) for 506 variable parameters by full-matrix least-squares refinement on F^2 reaches to $R_1 = 0.0650$ and $wR_2 = 0.1892$ with a goodness-of-fit of 0.991, the parameters *a* and *b* for weighting scheme are 0.1201 and 0. The final difference Fourier map shows maximum rest peaks and holes of 1.415 and −1.208 eÅ^{-3}, respectively.

3. Results and discussion

The dinuclear palladium complex **1** was obtained by modifications of literature procedures reported for the synthesis of branched palladium(II) alkynyl complexes [61,62] and linear rigid-rod metal-containing polyynes [32]. The formation of undesirable polymeric materials can be minimised by the slow addition of the alkynyl ligand to an excess of *trans*-[Pd(PEt_3)$_2$Cl$_2$] in the presence of copper(I) catalyst at low temperature to obtain the air and moisture stable complex **1** in good yield. Subsequent reactions to substitute the chloro ligands in complex **1** with various alkynyl ligands gave mixtures of complexes and oligomeric materials probably due to the lability of the palladium(II) metal centre.

The replacement of the chloro ligands in a versatile precursor complex [{ClPt(PEt_3)$_2$C≡C}$_2$-3,6-^{n}BuCarb-9] with various alkynyl ligands yielded the bis-alkynyl complexes **2**–**5** which were synthesized through the dehydrohalogenation reaction for the formation of platinum(II) alkynyl complexes [53], using trialkylamine as the base and Cu(I) halide as the catalyst with subsequent purification by column chromatography to afford air and moisture stable complexes **2**–**5**. Subsequent recrystallisation of the complexes gave analytically pure off-white to yellow microcrystalline solids.

All newly synthesized complexes have been characterised by ^{1}H NMR spectroscopy, IR spectroscopy and mass spectrometry, and gave satisfactory elemental analyses. Complexes **1**–**5** have also been characterised by $^{31}P\{^1H\}$ NMR spectroscopy. The X-ray crystal structures of **1** and **5** have also been determined.

The perspective drawings of complexes **1** and **5** are shown in Figs. 1 and 2, respectively. The selected bond distances and angles are tabulated in Table 1.

The palladium atoms in the X-ray structure of complex **1** showed the expected *trans*-square planar coordination geometry with a slight distortion, in which the P–Pd–Cl bond angles are in the range of 92.24(13)–93.43(12)°. The slight distortion from an ideal square-planar arrangement could be a result of the steric interactions

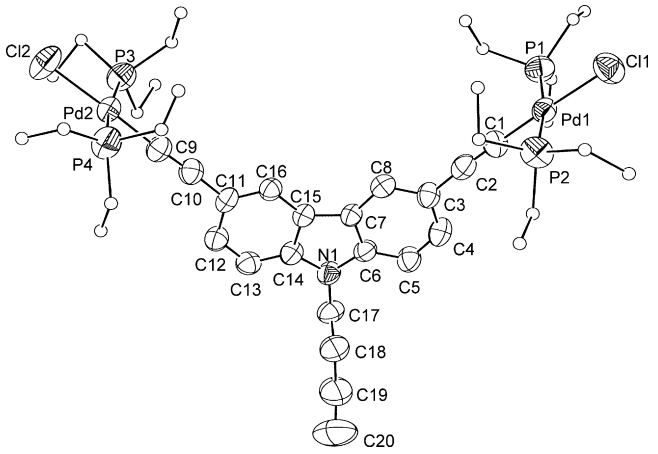

Fig. 1. Perspective view of **1** with atomic numbering scheme. Hydrogen atoms have been omitted for clarity. Thermal ellipsoids are shown at 30% probability level.

between the bulky ligands about the palladium(II) metal centres [61,62]. The coordination planes about the metal centres form interplanar angles of 89.0° and 89.2° with the carbazole backbone in **1**. This nearly orthogonal out-of-plane twisting of the coordination planes about the palladium atoms in **1** has also been previously observed in other palladium or platinum σ-alkynyl complexes [47,49,53,54,61,62]. In complex **1**, the bond distances of the Pd–C (1.899(1)–1.933(11) Å), as well as the C≡C (1.221(13)–1.253(14) Å) bond are found to be within the normal ranges for palladium(II) alkynyl complexes [61].

The structural features of complex **5** are comparable to those in the precursor complex [{ClPt(PEt_3)$_2$C≡C}$_2$-3,6-^{n}BuCarb-9]. The bond angles between the alkynyl ligand and the platinum metal centres are in the range of 174.8(15)–176.8(16)° and are close to the ideal of 180° for sp hybridized carbon, further confirming the σ-bonded nature of the alkynyl groups. The coordination planes of complex **5** are essentially square planar with slight distortions, with the P–Pt–C bond angles in the range of 86.5(5)–93.3(4)°, again, probably due to relief of steric hindrance from the presence of bulky ligands about the platinum(II) metal centres. Similar to that observed in complex **1**, the coordination planes about each platinum atom are not co-planar with the carbazole backbone with interplanar angles of 74.9° and 85.5°, which are similar to those found in the crystal structure of [{ClPt(PEt_3)$_2$C≡C}$_2$-3,6-^{n}BuCarb-9] [54] and other related platinum(II) bis-alkynyl mononuclear complexes of *trans*-[Pt(C≡CAr)$_2$(PEt_3)$_2$] [71]. No intermolecular π···π stacking interaction was observed between the planar pyrene moieties due to the presence of the bulky neighbouring trialkylphosphine ligands.

The slightly longer Pt–C bond distances found in complex **5** (1.979(18)–2.032(18) Å) compared to those in [{ClPt(PEt_3)$_2$C≡C}$_2$-3,6-^{n}BuCarb-9] (1.87(3) and 1.97(3) Å) are probably due to the stronger *trans* influence as a consequence of the presence of the

Table 1
Selected bond distances (Å) and bond angles (°) with estimated standard deviations (E.S.D.S.) in parentheses for **1** and **5**.

Complex **1**			
Selected bond distances (Å)			
Pd(1)–C(1)	1.899(1)	Pd(2)–P(3)	2.303(3)
Pd(1)–P(2)	2.286(3)	Pd(2)–P(4)	2.304(4)
Pd(1)–P(1)	2.305(3)	Pd(2)–Cl(2)	2.340(3)
Pd(1)–Cl(1)	2.348(3)	C(1)–C(2)	1.253(14)
Pd(2)–C(9)	1.933(11)	C(9)–C(10)	1.221(13)
Selected bond angles (°)			
C(1)–Pd(1)–P(2)	87.8(3)	P(3)–Pd(2)–P(4)	172.10(13)
C(1)–Pd(1)–P(1)	86.3(3)	C(9)–Pd(2)–Cl(2)	177.0(3)
P(2)–Pd(1)–P(1)	171.30(14)	P(3)–Pd(2)–Cl(2)	92.24(13)
C(1)–Pd(1)–Cl(1)	177.6(3)	P(4)–Pd(2)–Cl(2)	92.85(13)
P(2)–Pd(1)–Cl(1)	92.76(12)	Pd(1)–C(1)–C(2)	176.1(10)
P(1)–Pd(1)–Cl(1)	93.43(12)	C(1)–C(2)–C(3)	175.8(12)
C(9)–Pd(2)–P(3)	87.5(3)	Pd(2)–C(9)–C(10)	176.7(10)
C(9)–Pd(2)–P(4)	87.8(3)	C(9)–C(10)–C(11)	177.2(12)
Complex **5**			
Selected bond distances (Å)			
Pt(1)–C(1)	2.018(17)	Pt(2)–P(3)	2.309(5)
Pt(1)–C(21)	2.02(2)	Pt(2)–P(4)	2.312(5)
Pt(1)–P(1)	2.329(4)	C(1)–C(2)	1.23(2)
Pt(1)–P(2)	2.329(4)	C(9)–C(10)	1.218(19)
Pt(2)–C(39)	1.979(18)	C(21)–C(22)	1.22(2)
Pt(2)–C(9)	2.032(18)	C(39)–C(40)	1.23(2)
Selected bond angles (°)			
C(1)–Pt(1)–C(21)	175.3(6)	C(9)–Pt(2)–P(4)	89.6(5)
C(1)–Pt(1)–P(1)	87.7(4)	P(3)–Pt(2)–P(4)	175.5(2)
C(21)–Pt(1)–P(1)	93.3(4)	C(2)–C(1)–Pt(1)	175.2(14)
C(1)–Pt(1)–P(2)	88.3(4)	C(1)–C(2)–C(3)	177.8(17)
C(21)–Pt(1)–P(2)	90.9(5)	C(10)–C(9)–Pt(2)	176.1(15)
P(1)–Pt(1)–P(2)	175.59(16)	C(9)–C(10)–C(11)	177.8(17)
C(39)–Pt(2)–C(9)	178.2(7)	C(22)–C(21)–Pt(1)	174.8(15)
C(39)–Pt(2)–P(3)	86.5(5)	C(21)–C(22)–C(23)	178(2)
C(9)–Pt(2)–P(3)	93.1(5)	C(40)–C(39)–Pt(2)	176.8(16)
C(39)–Pt(2)–P(4)	90.9(5)	C(39)–C(40)–C(41)	178.5(18)

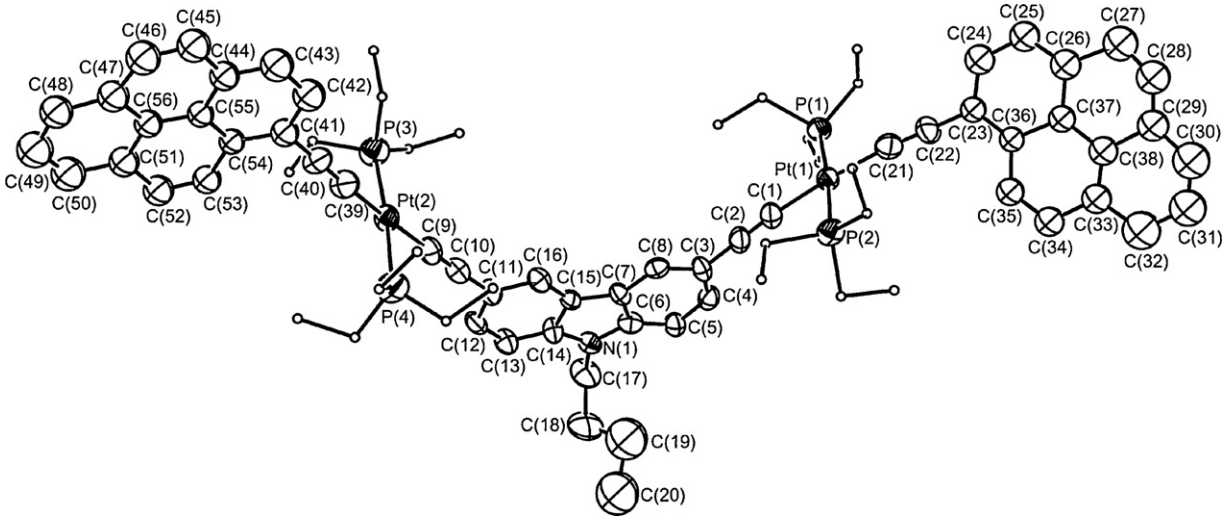

Fig. 2. Perspective view of **5** with atomic numbering scheme. Hydrogen atoms have been omitted for clarity. Thermal ellipsoids are shown at 30% probability level.

Table 2
Electronic absorption data of the carbazole-containing palladium(II) and platinum(II) alkynyl complexes in dichloromethane at 298 K.

Complex	λ/nm (ε/dm^3 mol^{-1} cm^{-1})
[{ClPd(PEt$_3$)$_2$C≡C}$_2$-3,6-^{n}BuCarb-9] (**1**)	258 (58,110), 268 (71,305), 280 sh (55,050), 310 sh (62,695), 316 (63,965), 348 sh (10,905), 364 sh (7,460), 382 (2,910)
[{MeOC$_6$H$_4$C≡CPt(PEt$_3$)$_2$C≡C}$_2$-3,6-^{n}BuCarb-9] (**2**)	262 (81,360), 290 (45,340), 302 sh (39,900), 334 sh (73,160), 354 (79,180), 392 sh (4,250)
[{MeC$_6$H$_4$C≡CPt(PEt$_3$)$_2$C≡C}$_2$-3,6-^{n}BuCarb-9] (**3**)	262 (82,700), 290 (48,890), 304 sh (41,880), 334 sh (75,150), 352 (77,510), 392 sh (3,810)
[{CF$_3$C$_6$H$_4$C≡CPt(PEt$_3$)$_2$C≡C}$_2$-3,6-^{n}BuCarb-9] (**4**)	260 (69,090), 270 sh (62,720), 294 (54,180), 306 sh (46,090), 332 (69,360), 356 (69,950), 394 sh (4,050)
[{PyrC≡CPt(PEt$_3$)$_2$C≡C}$_2$-3,6-^{n}BuCarb-9] (**5**)	292 (78,410), 332 (54,445), 372 (82,020), 388 (100,315), 402 (96,120)

second set of alkynyl groups in the bis-alkynyl complexes when compared to the chloro-alkynyl complexes.

The electronic absorption spectra of complexes **1**–**5** show intense absorption bands at 270–290 and 300–402 nm in dichloromethane solution. A summary of the electronic absorption spectral data is tabulated in Table 2.

The observation that the low-energy absorptions of complex **1** are red shifted relative to its *trans*-[Pd(PEt$_3$)$_2$Cl$_2$] precursor and diethynyl-3-6-butylcarbazole-9, together with the very large extinction coefficients that are much larger than those found in *trans*-[Pd(PEt$_3$)$_2$Cl$_2$], *trans*-[Pd(PEt$_3$)$_2$(C≡CR)$_2$] and *trans*-[Pd(PEt$_3$)$_2$(C≡CR)Cl] and very close to that of diethynyl-3-6-butylcarbazole-9, suggested that they are likely to be ligand-centred π–π^* transitions with metal perturbation. However, given the red shift in the absorption energies of these bands on going from **1** to [{ClPt(PEt$_3$)$_2$C≡C}$_2$-3,6-^{n}BuCarb-9], an involvement of a metal-to-alkynyl metal-to-ligand charge transfer (MLCT) transition is not unlikely. Previous reports by Masai et al. [72] also showed that low-energy metal-to-alkynyl MLCT absorptions are observed at *ca.* 300–360 nm in *trans*-[L$_2$M(C≡CR)$_2$] (L = tertiary phosphine or stilbine; M = Ni, Pd or Pt). For example, *trans*-[Pt(PEt$_3$)$_2$(C≡CH)$_2$] shows MLCT absorption bands at *ca.* 321 nm (log ε = 4.01) [72] in diethyl ether and at 304 nm

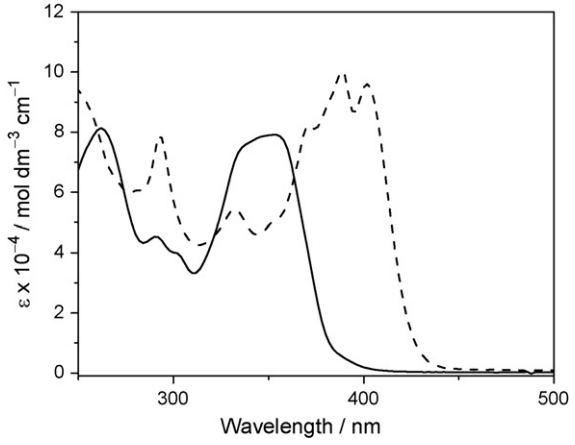

Fig. 3. Electronic absorption spectra of complexes **2** (—) and **5** (– – –) in dichloromethane at room temperature.

(ε = 7430 dm^3 mol^{-1} cm^{-1}) [73,74] in dichloromethane. Thus, the lowest energy absorption in **1** would best be described as a mixed $\pi \rightarrow \pi^*$IL/dπ(M) $\rightarrow \pi^*$(C≡CR) MLCT transition, with predominantly intra-ligand (IL) character. This assignment is further supported by the observation of a slight red shift in the lowest energy absorption band on going from a chloropalladium(II) alkynyl complex to its chloroplatinum(II) analogue [62]. Similarly, the absorption bands at 332–402 nm in complexes **2**–**5**, where the chloro ligands of [{ClPt(PEt$_3$)$_2$C≡C}$_2$-3,6-^{n}BuCarb-9] were substituted with other alkynyl ligands, are assignable as the $\pi \rightarrow \pi^*$IL/dπ(Pt) $\rightarrow \pi^*$(C≡CR) MLCT transition with predominant IL character. In particular, the electronic absorption spectrum of complex **5** shows vibrational progressional spacings that are characteristic of the pyrene moieties (Fig. 3). Slight red shifts in absorption bands were also observed for platinum(II) bis-alkynyl complexes **2**–**5** relative to their dichloro precursor complex, [3,6-{ClPt(PEt$_3$)$_2$C≡C}$_2$-9-^{n}BuCarb], probably due to the increased electron donation to the metal centre as well as the extended conjugation of the ground state through pπ–dπ overlap that led to a reduced IL/MLCT energy [39,40,53].

Complexes **2**–**5** show emission properties in dichloromethane solutions at room temperature while complexes **2**–**4** emit in the solid state at room temperature. In contrast, complex **1** shows emission properties in EtOH–MeOH (4:1, v/v) glass and in the solid state at 77 K. The emission data of all the complexes are summarised in Table 3.

Upon photo-excitation at $\lambda \geq 350$ nm at 77 K, the EtOH–MeOH (4:1, v/v) glass of **1** shows intense blue luminescence with rich vibronic structures at *ca.* 434 nm. The relatively large Stokes shifts, together with the emission lifetimes in the microsecond range are suggestive of their triplet parentage. Similar to the electronic absorption studies, the slight red shift of the emission energies on going from **1** to its chloroplatinum(II) analogue [{ClPt(PEt$_3$)$_2$C≡C}$_2$-3,6-^{n}BuCarb-9] would suggest there is certain degree of metal character in these emissions and should therefore be best described to emanate from a mixed $\pi \rightarrow \pi^*$(C≡CR) IL/dπ(Pt) $\rightarrow \pi^*$(C≡CR) MLCT triplet state with predominantly IL character. The non-emissive properties of the chloropalladium(II) at room temperature

Table 3
Photophysical data of the carbazole-containing platinum(II) and palladium(II) alkynyl complexes.

Complex	Medium (T/K)	λ_{em}/nm (τ_0/μs)
[{ClPd(PEt$_3$)$_2$C≡C}$_2$-3,6-^{n}BuCarb-9] (**1**)	CH_2Cl_2 (298)	–[a]
	Solid (298)	–[a]
	Solid (77)	482 (2.9)
	Glass (77)[b]	434 (32.8)
[{MeOC$_6$H$_4$C≡CPt(PEt$_3$)$_2$C≡C}$_2$-3,6-^{n}BuCarb-9] (**2**)	CH_2Cl_2 (298)	422 (<0.1)
	Solid (298)	503 (0.2)
	Solid (77)	503 (2.9)
	Glass (77)[b]	451 (56.2)
[{MeC$_6$H$_4$C≡CPt(PEt$_3$)$_2$C≡C}$_2$-3,6-^{n}BuCarb-9] (**3**)	CH_2Cl_2 (298)	426 (<0.1)
	Solid (298)	503 (0.3)
	Solid (77)	504 (3.1)
	Glass (77)[b]	450 (60.5)
[{CF$_3$C$_6$H$_4$C≡CPt(PEt$_3$)$_2$C≡C}$_2$-3,6-^{n}BuCarb-9] (**4**)	CH_2Cl_2 (298)	502 (<0.1)
	Solid (298)	494 (<0.1)
	Solid (77)	493 (2.0)
	Glass (77)[b]	450 (50.6)
[{PyrC≡CPt(PEt$_3$)$_2$C≡C}$_2$-3,6-^{n}BuCarb-9] (**5**)	CH_2Cl_2 (298)	657
	Solid (298)	–[a]
	Solid (77)	477
	Glass (77)[b]	655 (225)

[a] Non-emissive.
[b] Measured in EtOH/MeOH (4:1, v/v) glass.

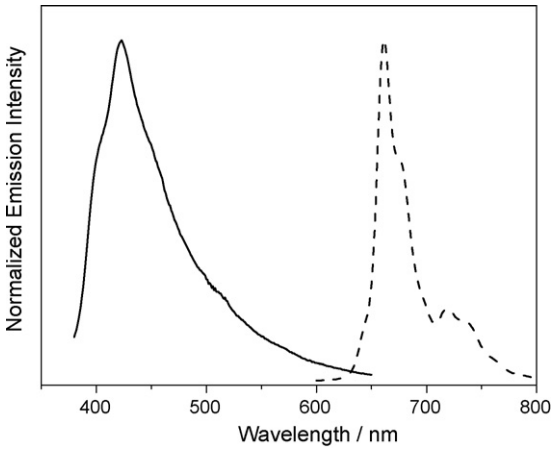

Fig. 4. Emission spectra of complexes **2** (—) and **5** (– – –) in dichloromethane at room temperature.

may be due to the presence of some effective low-lying non-radiative pathways, probably population of low-lying d–d ligand field (LF) states, which would impart their non-emissive behaviour. The presence of halide ligands, which are weak σ-donors, together with the fact that palladium being a second row transition metal element, would give rise to a small ligand-field splitting and thus the existence of low-lying d–d ligand-field states [75]. Moreover, in the case of palladium, additional low-lying halide-to-metal LMCT states are likely, which may lead to facile radiationless deactivation processes. Similar findings have previously been reported for *cis*- and *trans*-$[Pt(PEt_3)_2Cl_2]$ [73], where the *cis*–*trans* isomerisation observed has also been ascribed to the presence of their low-lying d–d excited states adopting tetrahedral rather than square-planar geometries [76]. In contrast to the non-emissive behaviour at room temperature of complex **1** and the platinum precursor complex [{ClPt(PEt$_3$)$_2$C≡C}$_2$-3,6-^{n}BuCarb-9], complexes **2**–**5** are found to emit in both dichloromethane solution and in the solid state at room temperature upon photo-excitation. Complexes **2**–**4** emit in the blue-green region with emission energies very similar to that observed for their precursor complex, [{ClPt(PEt$_3$)$_2$C≡C}$_2$-3,6-^{n}BuCarb-9] [54], in EtOH-MeOH (4:1, v/v) or in the solid state at 77 K and thus such emissions are similarly assigned to originate from a mixed $\pi \rightarrow \pi^*$(C≡CCarb) IL/dπ(Pt) $\rightarrow \pi^*$(C≡CCarb) MLCT triplet state with predominant IL character. It is likely that the low-lying non-emissive LF d–d states in [{ClPt(PEt$_3$)$_2$C≡C}$_2$-3,6-^{n}BuCarb-9] has been raised in energy upon substitution of the weak field chloro ligand with the strong field alkynyl ligand and therefore the bis-alkynyl complexes **2**–**4** are found to emit at room temperature. It is noteworthy that the emission energies of this series of complexes are nearly identical. Such insensitivity to the electronic inductive effect exerted by the substituents on the aryl-alkynyl ligands, together with their comparable excited state lifetimes to the precursor complex [{ClPt(PEt$_3$)$_2$C≡C}$_2$-3,6-^{n}BuCarb-9], would further confirm their emission origin. Similar ^{3}IL assignment has been suggested for a carbazole-containing metallopolymer [27].

Complex **5** are found to emit at longer wavelengths than **2**–**4** in dichloromethane solutions at room temperature upon photo-excitation (Fig. 4). The lower emission energy of **5** (655 nm) than **2**–**4** are suggestive of an emission origin that is of a different parentage from that of the other carbazole-containing platinum(II) bis-alkynyl complexes **2**–**4**. In view of the highly structured emissions of **5** with vibrational progressional spacings typical of pyrene moieties, they are assigned as originating predominantly from the ^{3}IL states of the corresponding ethynylpyrene units with some mixing of a dπ(Pt) $\rightarrow \pi^*$(C≡CPyr) ^{3}MLCT character. Similar emission profiles have also been observed in other pyrene-containing mononuclear platinum(II) alkynyl complexes with diimine or phosphine ligands [77].

Table 4
Electrochemical data for carbazole-containing platinum(II) and palladium(II) alkynyl complexes in dichloromethane at 298 K[a].

Complex	Oxidation E_{pa} (V vs. S.C.E.)[b]
[{ClPd(PEt$_3$)$_2$C≡C}$_2$-3,6-^{n}BuCarb-9] (**1**)	+0.90, +1.33
[{MeOC$_6$H$_4$C≡CPt(PEt$_3$)$_2$C≡C}$_2$-3,6-^{n}BuCarb-9] (**2**)	+0.70, +1.03, +1.18, +1.65
[{MeC$_6$H$_4$C≡CPt(PEt$_3$)$_2$C≡C}$_2$-3,6-^{n}BuCarb-9] (**3**)	+0.69, +1.12, +1.25, +1.62
[{CF$_3$C$_6$H$_4$C≡CPt(PEt$_3$)$_2$C≡C}$_2$-3,6-^{n}BuCarb-9] (**4**)	+0.74, +1.22, +1.40
[{PyrC≡CPt(PEt$_3$)$_2$C≡C}$_2$-3,6-^{n}BuCarb-9] (**5**)	+0.72, +1.03, +1.63, +2.10
[{ClPt(PEt$_3$)$_2$C≡C}$_2$-3,6-^{n}BuCarb-9]	+0.81, +1.24

[a] In dichloromethane (0.1M ^{n}Bu$_4$NPF$_6$); working electrode, glassy carbon; scan rate = 100 mVs^{-1}.
[b] E_{pa} refers to the anodic peak potential for the irreversible oxidation waves.

The electrochemical properties of the carbazole-containing platinum(II) and palladium(II) alkynyl complexes have been investigated by cyclic voltammetry and are summarised in Table 4.

There are no observable reduction waves for the carbazole-containing alkynylplatinum(II) phosphine complexes **1**–**5** upon reductive scan of up to –2.0 V vs. S.C.E. In the oxidative scan, the chloropalladium(II) alkynyl complex **1** shows irreversible oxidative waves at +0.90 and +1.33 V vs. S.C.E., while the platinum(II) complexes **2**–**5** generally show four irreversible oxidative waves at +0.69 to +0.74, +1.03 to +1.22, +1.18 to +1.40 and +1.62 to +2.10 V vs. S.C.E. With reference to previous studies on other carbazole-containing metal complexes and metallopolymers [27,29], together with the observation that a quasi-reversible couple that occurs at +0.91 V for diethynyl-3,6-butylcarbazole-9, the irreversible first oxidative waves at +0.90 V for complex **1** and +0.69 to +0.74 V vs. S.C.E. in complexes **2**–**5**, are probably due to the central palladium/platinum diethynylcarbazole moiety. In addition, the observation of a more positive first oxidation potential of complex **1** (+0.90 V) relative to that of its platinum analogue (+0.81 V) is also supportive of certain degree of metal-centred character in the HOMO, which is in line with the slight red shift in absorption and emission energies on going from the palladium complex to the platinum analogue. These observations are indicative of the highly mixed character of the HOMOs of this class of metal alkynyl complexes, probably due to the pπ–dπ overlap between the alkynyl ligand and the metal centre [42].

4. Conclusion

A series of luminescent carbazole-containing palladium(II) and platinum(II) alkynyl complexes have been successfully synthesized. Through a systematic comparison study, the emission of the platinum(II) bis-alkynyl complexes have been assigned to originate from an admixture of ^{3}IL/^{3}MLCT excited states with predominantly IL character. With the recent development of transition metal complexes in various fields in optoelectronics, such as OLEDs, optical limiters and materials with two-photon absorption and two-photon induced luminescence properties, these synthetically versatile carbazole-containing building blocks could serve as one of the attractive candidates in the construction of metal-containing functional materials.

Acknowledgements

V.W.-W.Y. acknowledges receipt of the Distinguished Research Achievement Award from The University of Hong Kong. We also acknowledge support from the University Development Fund and the Faculty Development Fund of The University of Hong Kong, The University of Hong Kong Foundation for Educational Development and Research Limited, and Strategic Research Theme on Molecular

Materials. The work described in this paper has been supported by a RGC Central Allocation Vote (CAV) Grant (HKU 2/05C). C.-H.T. acknowledges support from the University of Hong Kong and the receipt of a University Postdoctoral Fellowship.

References

[1] Y. Zhang, T. Wada, H. Sasabe, J. Mater. Chem. 8 (1998) 809.
[2] Y. Zhang, L. Wang, T. Wada, H. Sasabe, Appl. Phys. Lett. 70 (1997) 2949.
[3] X. Tao, Y. Zhang, T. Wada, H. Sasabe, H. Suzuki, T. Watanabe, S. Miyata, Adv. Mater. 10 (1998) 226.
[4] Y. Zhang, T. Wada, L. Wang, H. Sasabe, Chem. Mater. 9 (1997) 2798.
[5] G. Brizius, S. Kroth, U.H.F. Bunz, Macromolecules 35 (2002) 3517.
[6] S. Maruyama, H. Hokari, X. Tao, A. Gunji, T. Wada, H. Sasabe, Chem. Lett. (1999) 731.
[7] S. Maruyama, X. Tao, H. Hokari, T. Noh, Y. Zhang, T. Wada, H. Sasabe, H. Suzuki, T. Watanabe, S. Miyata, J. Mater. Chem. 9 (1999) 893.
[8] Z. Zhu, J.S. Moore, Macromolecules 33 (2000) 801.
[9] Z. Zhu, J.S. Moore, J. Org. Chem. 65 (2000) 116.
[10] G.A. Sotzing, J.L. Reddinger, A.R. Katritzky, J. Soloducho, R. Musgene, J.R. Reynolds, P.J. Steel, Chem. Mater. 9 (1997) 1578.
[11] V.I. Shishkina, Chem. Abstr. 78 (1973) 43188v.
[12] Y. Zhang, T. Wada, H. Sasabe, J. Polym. Sci., Part A: Polym. Chem. 34 (1996) 2289.
[13] Y. Zhang, T. Wada, L. Wang, H. Sasabe, J. Polym. Sci., Part A: Polym. Chem. 35 (1997) 685.
[14] M.S. Ho, C. Barrett, J. Paterson, M. Esteghamatran, A. Natansohn, P. Rochan, Macromolecules 30 (1997) 4613.
[15] Y. Zhang, T. Wada, L. Wang, T. Aoyama, H. Sasabe, Chem. Commun. (1996) 2325.
[16] Y. Zhang, L. Wang, T. Wada, H. Sasabe, Macromol. Chem. Phys. 97 (1996) 1877.
[17] G.H. Wang, C.W. Yuan, H.W. Wu, Y. Wei, J. Appl. Phys. 78 (1995) 2679.
[18] X. Tao, Y. Zhang, T. Wada, H. Sasabe, Appl. Phys. Lett. 71 (1997) 1921.
[19] D.B. Romero, F. Nüesch, T. Benazzi, D. Adés, A. Siove, L. Zuppiroli, Adv. Mater. 9 (1997) 1158.
[20] J.F. Wang, Y. Kawabe, S.E. Shaheen, M.M. Morrell, E. Jabbour, P.A. Lee, J. Anderson, N.R. Armstrong, B. Kippelen, E.A. Mash, N. Peyghambarian, Adv. Mater. 10 (1998) 230.
[21] C.I. Chao, S.A. Chen, Appl. Phys. Lett. 73 (1998) 426.
[22] E.G. Thianche, C. Sentein, A. Lorin, C. Denis, P. Raimond, J.M. Nunzi, J. Appl. Phys. 83 (1998) 4236.
[23] W.S. Bacsa, M. Schaer, L. Zuppiroli, D. Adés, A. Siove, J. Appl. Phys. 84 (1998) 5733.
[24] J. Kido, K. Hongawa, K. Okuyama, K. Nagai, Appl. Phys. Lett. 64 (1994) 815.
[25] A. Ribou, T. Wada, H. Sasabe, Inorg. Chim. Acta 288 (1999) 134.
[26] K.R.J. Thomas, J.T. Lin, Y. Lin, C. Tsai, S. Sun, Organometallics 20 (2001) 2262.
[27] W.Y. Wong, G.L. Lu, K.H. Choi, J.X. Shi, Macromolecules 35 (2002) 3506.
[28] N.S. Baek, H.K. Kim, E.H. Chae, B.H. Kim, J. Lee, Macromolecules 35 (2002) 9282.
[29] N.D. McClenaghan, R. Passalacqua, F. Loiseau, S. Campagna, B. Verheyde, A. Hameurlaine, W. Dehaen, J. Am. Chem. Soc. 125 (2003) 5356.
[30] M.S. Khan, R.K.M. Al-Saadi, L. Male, P.R. Raithby, J.K. Bjernemose, Acta Cryst. E59 (2003) m774.
[31] K. Sonogashira, S. Takahashi, N. Hagihara, Macromolecules 10 (1977) 879.
[32] S. Takahashi, M. Kariya, T. Yakate, K. Sonogashira, N. Hagihara, Macromolecules 11 (1978) 1063.
[33] S.J. Davis, B.F.G. Johnson, M.S. Khan, J. Lewis, J. Chem. Soc., Chem. Commun. (1991) 187.
[34] B.F.G. Johnson, A.K. Kakkar, M.S. Khan, J. Lewis, A.E. Dray, R.H. Friend, F. Wittman, J. Mater. Chem. 1 (1991) 485.
[35] M.S. Khan, A.K. Kakkar, N.J. Long, J. Lewis, P.R. Raithby, P. Nguyen, T.B. Marder, F. Wittmann, R.H. Friend, J. Mater. Chem. 4 (1994) 1227.
[36] D. Beljonne, H.F. Wittmann, A. Köhler, S. Graham, M. Younus, J. Lewis, P.R. Raithby, M.S. Khan, R.H. Friend, J.L. Brédas, J. Chem. Phys. 105 (1996) 3868.
[37] N. Chawdhury, A. Köhler, R.H. Friend, M. Younus, N.J. Long, P.R. Raithby, J. Lewis, Macromolecules 32 (1998) 722.
[38] N. Chawdhury, A. Köhler, R.H. Friend, W.Y. Wong, J. Lewis, M. Younus, P.R. Raithby, T.C. Corcoran, M.R.A. Al-Mandhary, M.S. Khan, J. Chem. Phys. 110 (1999) 4963.
[39] Y. Liu, S. Jiang, K. Glusac, D.H. Powell, D.F. Anderson, K.S. Schanze, J. Am. Chem. Soc. 124 (2002) 12412.
[40] K. Glusac, M.E. Köse, H. Jiang, K.S. Schanze, J. Phys. Chem. B 111 (2007) 929.
[41] E.C. Silverman, T. Cardolaccia, X. Zhao, K.-Y. Kim, K. Haskins-Glusac, K.S. Schanze, Coord. Chem. Rev. 249 (2005) 1491.
[42] J. Stahl, J.C. Bohling, E.B. Bauer, T.B. Peters, W. Mohr, J.M. Martín-Alvarez, F. Hampel, J.A. Gladysz, Angew. Chem. Int. Ed. 41 (2002) 1871.
[43] Q. Zheng, J.C. Bohling, T.B. Peters, A.C. Frisch, F. Hampel, J.A. Gladysz, Chem. Eur. J. 12 (2006) 6486.
[44] F. Zhuravlev, J.A. Gladysz, Chem. Eur. J. 10 (2004) 6510.
[45] G.-J. Zhou, W.-Y. Wong, Z. Lin, C. Ye, Angew. Chem. Int. Ed. 45 (2006) 6189.
[46] W.-Y. Wong, Dalton Trans. 40 (2007) 4495.
[47] S. Leininger, P.J. Stang, S. Huang, Organometallics 17 (1998) 3981.
[48] T.B. Marder, G. Lesley, Z. Yuan, H.B. Fyfe, P. Chow, G. Stringer, I.R. Jobe, N.J. Taylor, I.D. Williams, S.K. Kurtz, in: G.D. Stucky, S.R. Marder, J. Sohn (Eds.), Materials for Nonlinear Optics: Chemical Perspectives, ACS Symposium Series 455, American Chemical Society, Washington, DC, 1991, p. 605.
[49] N. Ohshiro, F. Takei, K. Onitsuka, S. Takahashi, Chem. Lett. (1996) 871.
[50] H. Lang, A. del Villar, J. Organomet. Chem. 670 (2003) 45.
[51] S.M. Al-Qaisi, K.J. Galat, M. Chai, D.G. Ray III, P.L. Rinaldi, C.A. Tessier, C.A. Youngs, J. Am. Chem. Soc. 120 (1998) 12149.
[52] K. Onitsuka, S. Yamamoto, S. Takahashi, Angew. Chem. Int. Ed. 38 (1999) 174.
[53] C.H. Tao, N. Zhu, V.W.-W. Yam, Chem. Eur. J. 11 (2005) 1647;
C.H. Tao, N. Zhu, V.W.-W. Yam, Chem. Eur. J. 14 (2008) 1377.
[54] C.H. Tao, K.M.-C. Wong, N. Zhu, V.W.-W. Yam, N. J. Chem. 27 (2003) 150.
[55] T.J. McKay, J.A. Bolger, J. Staromlynska, J.R. Davy, J. Chem. Phys. 108 (1998) 5537.
[56] R. Vestberg, R. Westlund, A. Eriksson, C. Lopes, M. Carlsson, B. Eliasson, E. Glimsdal, M. Lindgren, E. Malmström, Macromolecules 39 (2006) 2238.
[57] J.E. Rogers, J.E. Slagle, D.M. Krein, A.R. Burke, B.C. Hall, A. Fratini, D.G. McLean, P.A. Fleitz, T.M. Cooper, M. Drobizhev, N.S. Makarov, A. Rebane, K.-Y. Kim, R. Farley, K.S. Schanze, Inorg. Chem. 46 (2007) 6483.
[58] C.H. Tao, H. Yang, N. Zhu, V.W.-W. Yam, S.-J. Xu, Organometallics 27 (2008) 5453.
[59] V.W.-W. Yam, Acc. Chem. Res. 35 (2002) 555.
[60] V.W.-W. Yam, Chem. Commun. (2001) 789.
[61] V.W.-W. Yam, L. Zhang, C.H. Tao, K.M.-C. Wong, K.-K. Cheung, J. Chem. Soc., Dalton Trans. (2001) 1111.
[62] V.W.-W. Yam, C.H. Tao, L. Zhang, K.M.-C. Wong, K.-K. Cheung, Organometallics 20 (2001) 453.
[63] V.W.-W. Yam, K.M.-C. Wong, N. Zhu, J. Am. Chem. Soc. 124 (2002) 6506.
[64] S.K. Yip, E.C.-C. Cheng, L.-H. Yuan, N. Zhu, V.W.-W. Yam, Angew. Chem. Int. Ed. 43 (2004) 4954.
[65] V.W.-W. Yam, K.M.-C. Wong, L.-L. Hung, N. Zhu, Angew. Chem. Int. Ed. 44 (2005) 3107.
[66] T. Okano, M. Iwahara, H. Konish, J. Kiji, J. Organomet. Chem. 346 (1988) 267.
[67] Z. Otwinowski, W. Minor, Processing of X-ray diffraction data collected in oscillation mode, in: C.W. Carter Jr., R.M. Sweet (Eds.), Methods in Enzymology, vol. 276: Macromolecular Crystallography, Part A, Academic Press, 1997, pp. 307–326.
[68] G.M. Sheldrick, *SHELXS97*, Programs for Crystal Structure Analysis (Release 97-2). University of Goetingen, Germany, 1997.
[69] G.M. Sheldrick, *SHELXL97*, Programs for Crystal Structure Analysis (Release 97-2). University of Goetingen, Germany, 1997.
[70] A. Altomare, M.C. Burla, M. Camalli, G. Cascarano, C. Giacovazzo, A. Guagliardi, A.G.G. Moliterni, G. Polidori, R. Spagna, Sir97: a new tool for crystal structure determination and refinement, J. Appl. Cryst. 32 (1998) 115.
[71] J.P. Carpenter, C.M. Lukehart, Inorg. Chim. Acta 190 (1991) 7.
[72] H. Masai, K. Sonogashira, N. Hagihara, Bull. Chem. Soc. Jpn. 44 (1971) 2226.
[73] L. Sacksteder, E. Baralt, B.A. DeGraff, C.M. Lukehart, J.N. Demas, Inorg. Chem. 30 (1991) 2468.
[74] C.L. Choi, Y.F. Cheng, C. Yip, D.L. Phillips, V.W.W. Yam, Organometallics 19 (2000) 3192.
[75] C.K. Jørgensen, Prog. Inorg. Chem. 12 (1970) 101.
[76] P. Haake, T.A. Hylton, J. Am. Chem. Soc. 84 (1962) 3774.
[77] I.E. Pomestchenko, C.R. Luman, M. Hissler, R. Ziessel, F.N. Castellano, Inorg. Chem. 42 (2003) 1394.